Journal of Hydrology 529 (2015) 816–829

Contents lists available at ScienceDirect

Journal of Hydrology

journal homepage: www.elsevier.com/locate/jhydrol

RunCA: A cellular automata model for simulating surface runoff at different scales

Qi Shao [a,*], Dion Weatherley [b], Longbin Huang [a], Thomas Baumgartl [a]

[a] Centre for Mined Land Rehabilitation, Sustainable Minerals Institute, The University of Queensland, Brisbane, Queensland, Australia
[b] Julius Kruttschnitt Mineral Research Centre, Sustainable Minerals Institute, The University of Queensland, Brisbane, Queensland, Australia

ARTICLE INFO

Article history:
Received 3 August 2014
Received in revised form 28 August 2015
Accepted 1 September 2015
Available online 9 September 2015
This manuscript was handled by Konstantine P. Georgakakos, Editor-in-Chief, with the assistance of Ehab A. Meselhe, Associate Editor

Keywords:
Runoff modeling
Cellular automata
Model validation
Scale
Infiltration

SUMMARY

The Runoff Model Based on Cellular Automata (RunCA) has been developed to simulate surface runoff at different scales by integrating basic cellular automata (CA) rules with fundamental measureable hydraulic properties. In this model, a two-dimensional lattice composed of a series of rectangular cells was employed to cover the study area. Runoff production within each cell was simulated by determining the cell state (height) that consists of both cell elevation and water depth. The distribution of water flow among cells was determined by applying CA transition rules based on the minimization-of-difference algorithm and the calculated spatially varied flow velocities. RunCA was verified and validated by three steps. Good agreement with the analytical solution was achieved under simplified conditions in the first step. Then, results from runoff experiments on small laboratory plots (2 m × 1 m) showed that the model was able to well predict the hydrographs, with the mean Nash–Sutcliffe efficiency greater than 0.90. RunCA was also applied to a large scale site (Pine Glen Basin, USA) with data taken from literature. The predicted hydrograph agreed well with the measured results. Simulated flow maps in this basin also demonstrated the model capability in capturing both the spatial and temporal variations in the runoff process. Model sensitivity analysis results showed that the calculated total runoff and total infiltration were most sensitive to the input parameters representing the final steady infiltration rate at both scales. The Manning's roughness coefficient and the setting of cell size did not affect the results much at the small plot scale, but had large influences at the large basin scale.

1. Introduction

Surface runoff and associated soil erosion are subjects of continuous concern around the world, as they may have serious environmental consequences, including flood, landform instability (e.g., landslide and debris flow), loss of top soil and fertilizer leading to plant death or crop failure, and the transport of pollutants to surrounding areas and water courses. A quantitative evaluation of the extent and magnitude of runoff problems is consequently required to find, implement or improve land management strategies. For this purpose, some lumped conceptual runoff models have been developed since the 1970s, typical examples being the SCS curve number (U.S. Department of Agriculture, 1972), USLE (Wischmeier and Smith, 1978), CREAMS (Knisel, 1980) and RUSLE (Renard et al., 1997). These models usually treat the study area as a spatially singular entity, use state variables that represent averages over the entire area, and produce outputs at a single point according to empirical relationships (Haan et al., 1982). These models are computationally very efficient in calculating runoff and have relatively few input parameters. However, they are not able to capture the spatial or temporal variations in hydrological processes, and require calibration if applied to regions different from the location of first development.

To better describe the extent of spatial and temporal variability of runoff processes, some distributed physically based hydrologic models have emerged. Some of these models, including KINEROS (Smith, 1981), WEPP (Laflen et al., 1991), EUROSEM (Morgan et al., 1998b) and HEC-1 (Feldman, 1995), partition the target area (e.g., a catchment) using a network of elemental sections, such as a cascade of planes and channels. These elements are always simplified geometries with large sizes, which can provide a representation of the gross topographic features but may lose some local topography details and complexities. With the development of remote sensing, digital elevation models (DEMs) and geographic information systems (GIS), grid structures are more frequently used in hydrologic models, with examples being ANSWERS

* Corresponding author at: Level 5, Building 47A, The University of Queensland, Brisbane, Queensland 4072, Australia. Tel.: +61 411343092.
E-mail address: q.shao@uq.edu.au (Q. Shao).

http://dx.doi.org/10.1016/j.jhydrol.2015.09.003
0022-1694/

(Beasley et al., 1980), AGNPS (Young et al., 1989), LISEM (De Roo et al., 1996) and SHE (Abbott et al., 1986). These grids usually have much smaller sizes than the geometric elements and provide an easier way to represent the study area.

Numerical techniques have been widely employed in these distributed models to simulate the runoff routing processes. Typically, the overland flow and channel flow are described by solving the Saint–Venant equations of continuity and momentum. To make these complex equations solvable, simplifying assumptions need to be made and different methods are produced by neglecting various terms of the momentum equation (Chaudhry, 1993; Swensson, 2003). The kinematic wave model is the simplest method that neglects both acceleration and pressure terms, while the diffusion wave model is a more complete form that includes the influence of the pressure force (Chow et al., 1988). Therefore, the diffusion wave method is expected to be more accurate under complex conditions but at the expense of the reduced efficiency in computation. These two models only simulate the one-dimensional flow, while the spatial variation in the direction perpendicular to the principle slope could not be captured (MacArthur and DeVries, 1993; Vieux, 1991). The more advanced 2-D diffusion wave method, such as that used in CASC2D (Rojas et al., 2003), could better describe the spatial variation of the flow behaviors, but this would further increase the complexity and hence may lead to low computational efficiency.

Alternatively, several simpler methods have been developed for determining the water flows based on the elevation differences of the elements. For example, in AGNPS flow directions are determined from the DEM. The DEM-based runoff routing algorithms include both single-direction algorithms (e.g., D8 (O'Callaghan and Mark, 1984) and ρ8 (Fairfield and Leymarie, 1991)) that transfer all flow from the center grid to one downslope neighbor, and multiple-direction algorithms (e.g., MFD (Quinn et al., 1991), DEMON (Costa-Cabral and Burges, 1994) and D∞ (Tarboton, 1997)) that partition flow to multiple downslope neighbors. These elevation-based methods are very straightforward and computationally efficient; however, a major limitation is that they tend to be oversimplified as the water component in the elements is not taken into account. In reality, the water does not always flow according to the elevation differences because of the different water depths among the elements. Moreover, flow directions derived from these methods are pre-determined and fixed, thus nor the dynamic flow behaviors or the interactions between elements can be captured.

Therefore, alternative methods that have both high reliability and reduced complexity are required for more efficient hydrologic modeling. Cellular Automata (CA), a discrete dynamic system composed of a set of cells in a regular spatial lattice, is one of such promising approach worthy of investigation. Since the states of each cell depend only on the states of its neighbors and the global behavior of the whole system is determined by the synchronous evolution of all the cells in discrete time steps, CA is very effective in simulating dynamic complex natural phenomena from local to global according to simple transition rules (Wolfram, 1984). Unlike some other disciplines where CA has been widely applied and accepted, CA was not introduced into hydrology until Murray and Paola (1994) developed the first cellular braided river model about 40 years after CA was first proposed in the 1950s (Von Neumann, 1966). Later it was successfully applied to other hydrological processes, such as water flow in unsaturated soil (Folino et al., 2006; Mendicino et al., 2006) and ground water modeling (Ravazzani et al., 2011). However, only in the recent decade a few studies have emerged to relate its application to surface runoff modeling. For example, Mendicino et al. (2013) added an overland flow module to their CA based ecohydrological model (Cervarolo et al., 2011). While their model takes the advantage of CA that is directly compatible with the efficient parallel computing, the runoff routing process is still determined by the diffusion wave model. Rinaldi et al. (2007) and Ma et al. (2009) also developed CA based algorithms for simulating runoff in large plains and on hill-slopes, respectively. Both models have shown the capacity of CA, however, a spatially uniform flow velocity was assumed and simply applied over the entire study area, leading them to be only used for simulating the steady flow conditions. Parsons and Fonstad (2007) developed a more complex CA model capable of simulating the unsteady flow conditions by delaying the water from one cell to the next until the correct timing is reached. Although this is a significant progress, unfortunately in their model the flow directions were restricted to only four cardinal directions due to the difficulties in producing accurate timed water flows. Uncertainty also existed in selecting an appropriate time step for simulation. In addition, calculation of the rainfall excess is rather simple and empirical in this model as it does not include any related hydrologic principles. Some other CA models, such as RillGrow (Favis-Mortlock, 1998), EROSION-3D (Schmidt et al., 1999), and CAESAR (Coulthard et al., 2000), incorporate a surface hydrology component, but it is usually simplified because these models were primarily developed to study soil erosion or landform evolution. Consequently, in this study a CA-based model, which integrates measurable hydrologic parameters, is developed for quantitatively predicting the dynamic surface runoff processes under complex conditions at different scales. The efficacy of this model is then validated by the analytical solution under simplified conditions, the laboratory experiments at small plot scale and the field measurements at large basin scale. Sensitivity analysis is also conducted to understand the model response to input parameters and model settings.

2. Model development

A typical CA based model A can be expressed as a quadruple (Gregorio and Serra, 1999):

$$A = (Z^d, X, S, \sigma) \quad (1)$$

where Z^d represents a lattice of cells covering the study area, X is the definition of the local neighborhood, S is the set of cell states, and σ is the transition rule determining the changes in cell properties. Based on this structure and integrated with the physical processes involved in runoff production and distribution, the RunCA (Runoff Model Based on Cellular Automata) has been developed and is described as follows.

2.1. Definition of lattice space and spatial cells: partition process

As illustrated in Fig. 1, in this model the study area is partitioned into small hydrologic elements by a two-dimensional lattice consisting of square cells. This discretization is selected for its simplicity, broad application and convenience of implementation in

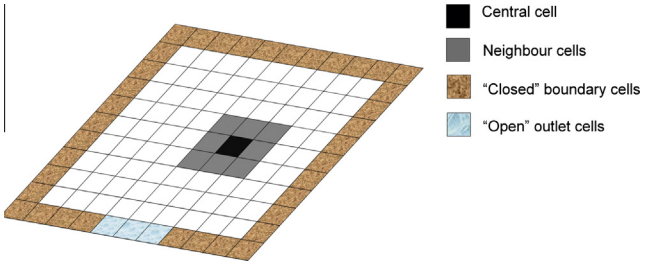

Fig. 1. Lattice space and spatial cells in the RunCA model.

computers. The model uses the Moore-neighborhood, which consists of eight adjacent cells in the four cardinal directions and the four diagonal directions from the center cell. The spatial cells located on the borders of the lattice space are treated as "closed and reflective" cells that simulate virtual plot boundaries. No water flows beyond these boundary cells. The cells located at the outlet are treated as "open and absorbing" cells, which means they will absorb any water flowing into them by moving the water into a storage value. These values can then be used to track the volume of water leaving the study area and thus record the runoff amount as a virtual runoff collector.

The simulation accuracy and computational complexity of CA models are largely determined by the size of their spatial cells, which is affected by various factors, including the size and spatial homogeneity of the study area, model accuracy requirements and the resolution of available spatial data (e.g., resolution of DEM/GIS maps and density of rain gauges). Typically, the accuracy of results can be improved by reducing the cell size, however, at the expense of increased time and computational resources required to run the model.

2.2. Determination of cell state: runoff production process

At each time step, the simulation of the runoff production process is based on the determination of the cell state, expressed as the cell height, which consists of both cell elevation and water depth. The cell elevation is derived from field measurements, topographic maps or DEM, and remains constant during a rainfall event. The determination of water depth is relatively complex, as it varies both temporally and spatially, and is controlled by both the effective rainfall at the current time step and the balance between inflows and outflows at the last time step, derived from transition rules described later. The effective rainfall (R_e) is determined by three components in Eq. (2):

$$R_e = R_i - P - I \tag{2}$$

where R_e is input rainfall, P is interception by vegetation, and I is infiltration. Here the evapotranspiration is neglected because it is negligible during runoff-producing rainfall events. In order to obtain the effective rainfall, it is necessary to quantitatively characterize all three components.

2.2.1. Input rainfall (R_i)

The input rainfall information at each time step can be derived from local measurements using rain gauges and/or records from nearby meteorological stations. For small scale simulation (e.g., small hillslopes), rainfall can be assumed to be uniformly distributed over the study area. For large scales, the spatial distribution of rainfall needs to be considered and different rainfall inputs should be applied to different cells, for which spatial interpolation methods may be employed.

2.2.2. Interception (P)

Interception refers to the portion of input rainfall collected, stored and evaporated from vegetation. In the areas barren of vegetation, interception is negligible. However, its relative effect can be significant when the vegetation cover is high and the rainfall intensity is small. In this model, interception is determined by the method used in LISEM (De Roo et al., 1996), where the cumulative interception during a rainfall event is estimated using an equation developed by Aston (1979):

$$P_{cum} = P_{\max}\left[1 - \exp\left(-0.046LAI\frac{R_{cum}}{P_{\max}}\right)\right] \tag{3}$$

where P_{cum} is the cumulative interception (mm), R_{cum} is the cumulative rainfall (mm), LAI is the leaf area index, and $P_{\max}$ is the maximum interception storage capacity (mm) that can be estimated from LAI using the equation developed by Von Hoyningen-Huene (1981):

$$P_{\max} = 0.935 + 0.498LAI + 0.00575LAI^2 \tag{4}$$

From the cumulative interception, the interception increment at each time step (P) is calculated by subtracting the P_{cum} at a previous time step from that at the current time step.

2.2.3. Infiltration (I)

In many cases, infiltration prediction directly determines the accuracy of a hydrologic model, as it controls how much water will enter the unsaturated soil zone, and how much will flow on the ground surface as runoff. It is difficult to quantitatively analyze the infiltration process due to various factors affecting it and its changing characteristics with time, but several physically based and empirical infiltration models have been developed. Among these models, the Philip (1957), Green and Ampt (1911), Horton (1940) and Holtan (1961) equations (Table 1) are frequently used due to their simplicity, good fit to data and the ability to obtain their parameter values. These four infiltration models have been implemented in the RunCA model, permitting investigation of their relative efficacy for runoff prediction during single consecutive rainfall events (Table 1). However, these models are only valid when the water supply rate at all times exceeds the soil infiltration capacity as they were primarily developed for describing the infiltration processes under ponding conditions. They cannot be used for intermittent or multiple rainfall events, where the recovery of infiltration capacity during dry periods needs to be considered. To make the RunCA model applicable to complex rainfall conditions and long-term simulations, two improved infiltration models, including the modified Horton equation (Aron, 1992; Bauer, 1974) and the modified Holtan equation (Huggins and Monke, 1966, 1968), are incorporated to allow soil drainage and infiltration recovery (Table 1).

2.3. Application of transition rules: runoff distribution process

At each time step and after determining the states (i.e., water depth and cell height) of each cell, the redistribution of water among the spatial cells is then derived by applying three CA transition rules to all these cells.

Table 1
Infiltration equations integrated in RunCA.[a]

Single continuous rainfall events		Intermittent/multiple rainfall events	
Philip equation	$i_t = 0.5S_0t^{-0.5} + A$	Modified Horton equation	$i_t = i_0 + d_t - kS_t$
Green-Ampt equation	$i_t = K_s[\lambda/I_t + 1]$	Modified Holtan equation	$d_t = \frac{i_f}{i_0}kS_t$
Horton equation	$i_t = i_f + (i_0 - i_f)e^{-kt}$		$i_t = i_f + (i_0 - i_f)\left(\frac{S_t'}{\varphi D}\right)^P$
Holtan equation	$i_t = i_f + (i_0 - i_f)\left[\frac{S-I_t}{\varphi D}\right]^P$		$d_t = i_f\left[1 - \frac{S_t'}{(\varphi - FC)D}\right]^3$

[a] i_t: infiltration capacity at time t, mm/h ; S_0: sorptivity, mm $h^{-0.5}$; A: soil water transmissivity, mm/h; K_s: hydraulic conductivity at natural saturation, mm/h; λ: fitting parameter in Green-Ampt equation, mm; I_t: cumulative infiltration at time t, mm; i_f: final steady infiltration rate, mm/h; i_0: initial infiltration rate, mm/h; k: infiltration decay factor in Horton equation, h^{-1}; S: soil water storage potential, mm; φ: total porosity, %; D: control zone depth, mm; P: dimensionless coefficient relating decrease rate of infiltration capacity in Holtan equation; d_t: soil drainage rate at time t, mm/h; S_t: cumulative soil water at time t, mm; S_t': soil water storage potential at time t, mm.

2.3.1. 1st transition rule for identifying flowing neighbors

This first transition rule determines at each time step to which neighbor cells the water in each central cell will flow, on the basis of the minimization of differences algorithm. This algorithm was first proposed by Gregorio and Serra (1999), and is based on a very straightforward principle that a dynamic system tends to evolve towards equilibrium conditions by flow of some conserved quantity in the central cell to its neighbors. Specific to this runoff model, the water always flows from the central cell to its lower-height neighbor cells, in order to minimize the height differences among cells to reach equilibrium conditions. To implement this algorithm in RunCA, the average cell height in a local neighborhood area is firstly determined and compared to the height of each neighbor cell to eliminate the neighbors with larger height values. Then a new average height is calculated and again compared to the remaining neighbors for further elimination. This process repeats until no neighbor could be eliminated, and then the remaining neighbors are identified as the flowing neighbors that will receive water flows from the central cell. The more detailed procedure and the equations for calculation are shown in Fig. 2.

Three different flow-direction options are included in this model. The first one (4N) only allows the water in the central cell to flow to four cardinal neighbors, while the second option (8N) allows eight flow directions by including the four diagonal neighbors. However, according to the previous findings on the MFD (Multiple flow direction) DEM-based runoff routing algorithm, the 4N and 8N type tends to cause under flow divergence and over flow divergence, respectively (Erskine et al., 2006). Therefore, a third flow-direction option (4 + 4N) is proposed, which gives the water in a cell the priority to flow to its four cardinal neighbors,

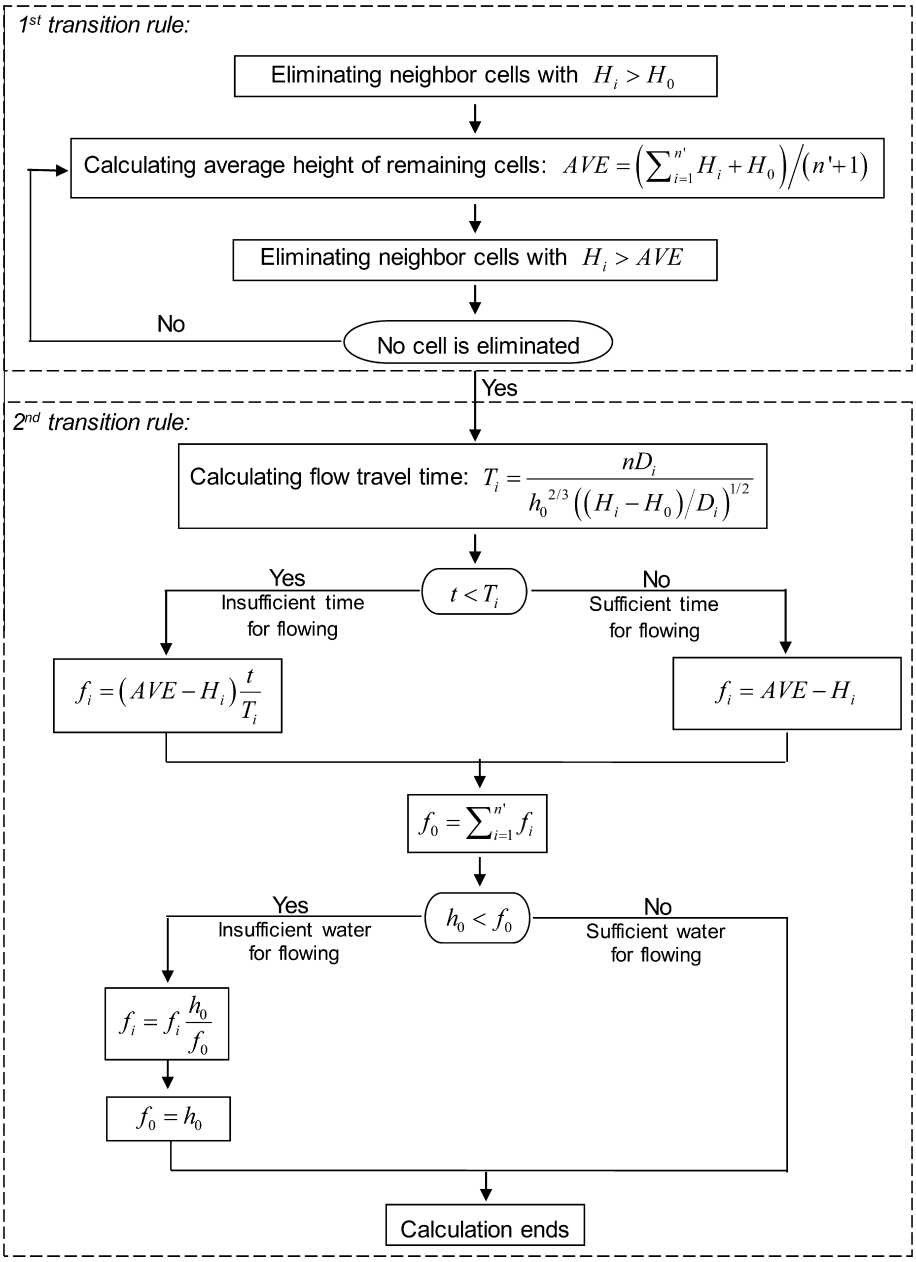

Fig. 2. Flowchart for calculating water flows from central cell to neighbors. H_i (mm) and H_0 (mm) represents neighbor heights and central cell height, respectively; n' is the number of remaining neighbors after each elimination; T_i (s) and D_i (m) represents flow travel time and distance from central cell to each flowing neighbor, respectively; n is Manning's coefficient; h_0 (mm) is the water depth in central cell; t (s) is time step; f_i (mm) represents the flow amount from central cell to each flowing neighbor, while f_0 (mm) is the total outflow from central cell.

and only allows it to flow to the four diagonal neighbors when there is no cardinal neighbor to flow to (i.e., all the cardinal neighbors are higher than the central cell). This is a compromise between the former two options, and is expected to be more realistic by controlling the flow dispersion and at the same time keeping the eight possible flow directions. Their performance will be evaluated and compared later in the model testing sections.

2.3.2. 2nd transition rule for calculating flow amount to flowing neighbors

According to the minimization of differences algorithm, the potential flow amount f_p (mm) from the central cell to each identified flowing neighbor is determined by the difference of its height and the average height. However, this calculation is based on the assumption of a constant velocity for all the flows. In reality the water flow velocity on a hillslope or in a catchment is spatially and temporally highly variable due to various conditions, such as local elevation gradient, surface roughness and water depth. These variations are essential for the runoff distribution, and thus are considered in RunCA by calculating the travel time for all the flows. Specifically, the Manning's equation is employed to determine the velocity V (m/s) for the outflow from the central cell to each flowing neighbor:

$$V = \frac{h^{2/3} s^{1/2}}{n} \tag{5}$$

where h (m) is water depth in the central cell, n is Manning's roughness coefficient, and s is water surface slope which is calculated from dividing the flow travel distance D (m) by the height difference of the central cell and its flowing neighbor. Then the time T (s) required for water to travel from the central cell to its flowing neighbor can be calculated from dividing the flow travel distance by the flow velocity, as shown in Eq. (6):

$$T = \frac{D}{V} = \frac{nD}{h^{2/3} s^{1/2}} \tag{6}$$

If L (m) represents the cell side length, then D equals to L and $\sqrt{2}L$, respectively for the cardinal flowing neighbor and the diagonal flowing neighbor. This definition considers the different distances from cardinal neighbors and diagonal neighbors to the central cell, thus allowing the mass conservation when the water flows to the neighbor cells.

The relationship between the calculated flow travel time T (s) and the time step t (s) used in the simulation determines whether there is sufficient time for the calculated f_p to finish travelling from a central cell to its neighbor cell. Therefore, the actual flow amount f (mm) in each time step is determined by Eq. (7):

$$f = \begin{cases} f_p, & t \geqslant T \\ f_p \frac{t}{T}, & t < T \end{cases} \tag{7}$$

This equation explains that when t is smaller than T, only a portion of f_p, which is equal to the ratio between t and T, can flow from a central cell to a neighbor cell. Based on this consideration, a small time step which is less than most of the calculated flow travel times is demanded. To estimate a suitable time step value, the potential flow travel times are calculated prior to the simulation, by assuming s equal to the land surface slope gradient and h equal to the elevation differences between cells. These calculated potential flow travel times are further sorted from largest to smallest and their percentiles are given, which provide a reference for the selection of time step. Normally a time step smaller than the 99% percentile is recommended to guarantee the simulation accuracy.

After determining the amount of each flow, the total outflow from each central cell f_0 (mm) is then calculated by the sum of f to all its flowing neighbors. When f_0 is larger than its water depth h_0 (mm), which means that the water in the central cell is not sufficient for all the calculated outflows, f to each flowing neighbor needs to be further modified by timing a ratio of h_0 and f_0. In this case the final f_0 is equal to h_0.

The detailed calculation process and equations used for this transition rule is demonstrated in the flowchart shown in Fig. 2.

2.3.3. 3rd transition rule for determining total flows

At each time step the former two transition rules are applied to all the spatial cells in the lattice space, thus the outflow f from each central cell to each of its neighbors can be determined and stored in a buffer. However in the global view, each central cell is also one neighbor of its adjacent cells, thus it not only flows water out, but also receives water from the surrounding cells at the same time. Consequently a third transition rule needs to be applied to calculate the total flow F (mm) (the balance between outflow and inflows) for each cell. This transition rule is based on the consideration that the inflows from the neighbors to each cell can be derived from the according outflows of these neighbors. More specifically, if i and j represent the row number and column number respectively, and the arrows represents the flow directions, then the total flow for the cell (i,j) can be determined by Eq. (8) for 4N option, and Eq. (9) for both 8N and 4 + 4N options:

$$F(i,j) = f(i-1,j)(\downarrow) + f(i,j-1)(\rightarrow) + f(i,j+1)(\leftarrow) + f(i+1,j)(\uparrow) - f_0(i,j) \tag{8}$$

$$F(i,j) = f(i-1,j-1)(\searrow) + f(i-1,j)(\downarrow) + f(i-1,j+1)(\swarrow) + f(i,j-1)(\rightarrow) + f(i,j+1)(\leftarrow) + f(i+1,j-1)(\nearrow) + f(i+1,j)(\uparrow) + f(i+1,j+1)(\nwarrow) - f_0(i,j) \tag{9}$$

The calculated total flow could be positive if the sum of inflows is larger than the total outflow, or reversely negative. Then the new water depth and cell height are updated by adding this total flow to the current water depth for the calculation of the next time step. This allows the simultaneous update of the states of all the cells.

Based on all the components discussed above, RunCA has been implemented in C++ using the object-oriented paradigm for the sake of flexibility and reusability. The model structure and modeling procedure is summarized in Fig. 3. Before applying the developed model to real cases, it must be tested and verified to ensure that the model indeed represents the physical world adequately. Therefore, a systematic verification and validation procedure consisting of three steps (Wang et al., 2009) was employed in this study: (1) verification by analytical solution under simplified conditions to test the physical basis of the model and to ensure the validity of computer coding and calculation algorithm; (2) validation by laboratory experiments to evaluate the model's capacity in reproducing the basic physical processes of surface runoff; and (3) validation by field measurements to prove that the model has the capability of predicting the behavior of the natural phenomenon.

Two standard statistical metrics, including Nash–Sutcliffe efficiency or modeling efficiency (*EF*) (Nash and Sutcliffe, 1970) and root mean square error (*RMSE*), were used to evaluate the performance of RunCA. *EF* describes the proportion of the variance of the observed values that is accounted for by the model, and its value can vary from 1 (perfect fit) to negative infinity. *RMSE* shows the amount of divergence of the model values from the observed values and its value close to 0 indicates good agreement. The mathematical expressions used for these two statistical analysis measures are:

$$EF = 1 - \frac{\sum_{i=1}^{n} (O_i - P_i)^2}{\sum_{i=1}^{n} \left(O_i - \overline{O}\right)^2} \tag{10}$$

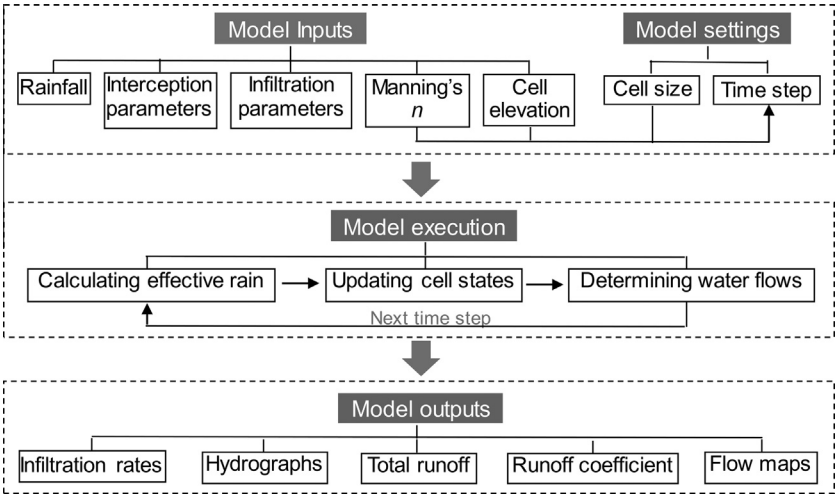

Fig. 3. Flowchart for RunCA modeling procedure.

$$RMSE = \sqrt{\frac{1}{n}\sum_{i=1}^{n}(O_i - P_i)^2} \quad (11)$$

where n is number of observations during the simulation period; O_i and P_i are observed and simulated values at each comparison point i; $\overline{O}$ is arithmetic mean of the observed values.

3. Model verification by analytical solution under simplified conditions

RunCA was firstly tested against the analytical solution for the idealized overland flow over a uniform plane using the kinematic wave modeling, as suggested by Singh (1996). A 500 m long and 100 m wide hypothetical flow plane at a uniform slope of 5% was considered, where the surface roughness, slope, and rainfall regime were assumed invariant in space and time. A Manning's n of 0.01, a cell size of 1 m and a time step of 1 s were set for all the simulations by RunCA in this section.

The effective rainfall of 100 mm/h was applied on an impervious plane with no infiltration, and the hydrographs predicted by both the analytical solution (derived from Figure 12.13 and 12.26 in Singh (1996)) and RunCA are shown in Fig. 4. Fig. 4a represents the equilibrium hydrograph where the rainfall duration is 25 min and is larger than the time of concentration, i.e., the time when flow from the farthest point reaches the outlet, while Fig. 4b shows the partial equilibrium hydrograph where the rainfall duration is 5 min and is smaller than the time of concentration. Both figures show that compared to the results derived from the analytical solution, RunCA predicted slightly higher values of runoff rates during the rising limbs while slightly lower values during the recession limbs of the hydrographs. However, they had very similar crest segments where the peak discharge rate values were almost the same. The large *EF* values (0.964 and 0.923) and small *RMSE* values (8.054 mm/h and 6.414 mm/h) indicated the good agreement between analytical solution and RunCA.

Fig. 4c and d shows the results for another case where the 120 mm/h of rainfall was applied on the infiltrating plane with a constant infiltration rate of 20 mm/h. Similarly, both equilibrium and partial equilibrium conditions were considered using the 25 min and 5 min rainfall durations. Again, good fit between the hydrographs based on the analytical solution (derived from Figure 13.10 and 13.18 in Singh (1996)) and RunCA was achieved. Hence, the model verification by the analytical solution of the equation of continuity and momentum verifies the transition rules

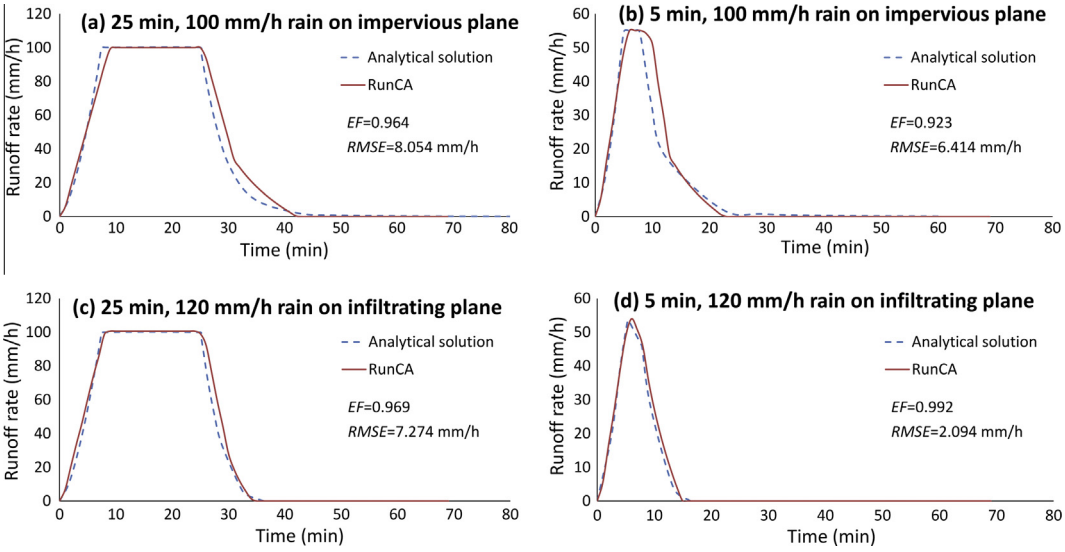

Fig. 4. Simulated hydrographs based on the analytical solution and RunCA, for both the impervious plane (a, b) with no infiltration and the infiltrating plane (c, d) with a constant infiltration rate of 20 mm/h.

for runoff distribution in RunCA and the correctness of the software code, and at the same time suggests the model ability in reflecting the basic physical processes involved in surface water flows.

4. Model validation with laboratory experiments at small plot scale

Laboratory experiments are often conducted in a controllable and repeatable environment, smaller in scale and less costly to measure more properties at higher resolution of the measuring points. Therefore, the comparison between the measured values with modeled results is more meaningful to test the model's capability in reproducing the most fundamental physical processes of the system tested (Wang et al., 2009; Wang and Wu, 2004). In this study, the performance of RunCA was tested by using the results of runoff experiments previously carried out at small plot scale in the rainfall simulation laboratory of Beijing Normal University, China.

4.1. Experimental data

Small laboratory plots (2 m × 1 m) were established by spraying the substrate, consisting of a mixture of natural soil and soil adhesive, onto a platform using the soil-spray technique to form a stabilized soil layer with a thickness of 30 cm (Fig. S1 of the Supplementary material). Six treatments were set up based on two different types (inorganic and polymer) and three contents (0.3%, 0.5%, 0.7%) of soil adhesives to achieve different infiltration characteristics among plots. Simulated rainfall was produced by a group of rainfall simulators (Fig. S1 of the Supplementary material), which use Veejet 80100 nozzles, with a water pressure of 0.04 MPa, height of 5 m, target area of 2.2 m × 3 m, and coefficient of uniformity of 95%. Steady rainfalls with three different intensities (20 mm/h, 44 mm/h and 70 mm/h) were applied to the plots at three different slope gradients (10%, 20% and 30%), with a duration of 2 h for each rainfall event.

Surface runoff has been collected and measured every five minutes during all the rainfall events. Measured total runoff volumes are summarized in Table S2 of the Supplementary material. Results showed that total runoff increased with increasing adhesive content within both groups of plots treated by inorganic and polymer adhesive, with the latter group tending to generate more runoff. In addition, larger runoff amount has been produced at steeper slopes and during higher intensity rainfall events.

4.2. Model inputs and settings

Before running RunCA for runoff simulation, five groups of input parameters needed to be determined, as well as two basic model settings (Fig. 3):

Cell elevation: due to the straight slope profile and the relative smooth surface, the elevation of each line of cells on the plot could be easily calculated based on the slope length and angle. After applying the rainfall using the simulator, some rills were observed on some plots. The elevation of the cells located on these rills were determined by subtracting the measured rill depths.

Rainfall: actual rainfall intensity was measured by tipping buckets for each rainfall event, and was considered homogeneously distributed on the plot because of the high coefficient of uniformity of rainfall simulators and the small size of the runoff plot.

Interception: this part was ignored since no vegetation cover existed on any plot.

Manning's n: this roughness coefficient was derived empirically from the guide values in EUROSEM (Morgan et al., 1998a). The resulted values varied from 0.026 for plot 1 treated with lowest content of inorganic adhesive to 0.016 for plot 6 treated with highest content of polymer adhesive.

Infiltration: infiltration rate of each plot varied temporally and the four infiltration equations for single rainfall events (Table 1) were selected due to the continuous rainfall applied. Since the input parameter values for these infiltration equations were not measured in this experiment, they were derived indirectly by calibration with the actual infiltration values, which were determined by subtracting measured runoff amount from rainfall amount every five minutes. For each plot at each slope gradient, infiltration parameters were calibrated by curve-fitting with the experimental data in the 44 mm/h rainfall event, and the calibrated values were then used for runoff simulations in both 20 mm/h and 70 mm/h rainfall events. Table 2 summarizes the derived parameter values,

Table 2
Calibrated infiltration parameter values and coefficients of determination (R^2) for curve-fitting results at small plot scale.[a]

Plot	Slope (%)	Philip			Horton				Green-Ampt			Holtan			
		A	S_o	R^2	i_f	i_0	k	R^2	K	a	R^2	i_f	i_0	P	R^2
1	10	1.34	0.44	0.85	1.33	2.50	1.65	0.97	1.50	0.05	0.79	1.24	2.62	1.03	0.96
	20	1.14	0.39	0.99	1.33	2.74	6.77	0.95	1.30	0.04	0.98	1.04	2.12	1.45	0.91
	30	0.83	0.35	0.91	0.98	2.79	7.48	0.94	1.03	0.04	0.87	0.82	3.68	2.53	0.94
2	10	1.24	0.44	0.73	0.98	2.37	1.38	0.99	1.41	0.05	0.59	1.02	3.02	1.20	0.99
	20	0.92	0.37	0.98	1.07	2.49	5.26	0.97	1.08	0.05	0.96	0.94	3.79	2.98	0.94
	30	0.69	0.34	0.91	0.88	2.63	9.29	0.95	0.87	0.04	0.88	0.69	3.51	2.72	0.93
3	10	0.92	0.46	0.76	0.49	2.30	1.58	0.99	1.12	0.06	0.62	0.59	5.77	2.29	0.99
	20	0.64	0.40	0.93	0.65	2.24	3.06	0.99	0.83	0.06	0.90	0.45	3.99	2.87	0.99
	30	0.44	0.35	0.92	0.64	2.42	8.57	0.98	0.60	0.05	0.88	0.30	4.21	3.28	0.94
4	10	1.26	0.44	0.84	1.36	2.30	1.24	0.93	1.41	0.05	0.78	1.12	2.12	0.71	0.90
	20	0.97	0.39	0.98	1.14	2.56	4.64	0.96	1.14	0.05	0.97	0.82	3.02	2.35	0.93
	30	0.69	0.35	0.88	0.80	2.67	6.90	0.94	0.89	0.05	0.85	0.71	3.58	2.55	0.94
5	10	1.24	0.45	0.55	1.00	2.20	0.97	0.98	1.38	0.29	0.74	0.94	2.45	0.83	0.97
	20	0.74	0.37	0.93	0.77	2.30	3.51	0.96	0.92	0.05	0.90	0.89	3.21	2.75	0.95
	30	0.52	0.33	0.86	0.62	2.45	6.55	0.94	0.72	0.05	0.81	0.80	3.24	2.72	0.94
6	10	0.89	0.43	0.83	0.79	1.95	1.16	0.96	1.04	0.06	0.75	0.82	2.63	1.42	0.95
	20	0.58	0.38	0.94	0.61	2.07	2.73	0.97	0.76	0.06	0.92	0.59	2.91	2.53	0.96
	30	0.31	0.33	0.87	0.49	2.30	7.74	0.97	0.47	0.05	0.83	0.49	3.14	3.06	0.94
Mean				0.87				0.96			0.84				0.94

[a] All the symbols representing infiltration parameters are the same as those in Table 1.

with the mean coefficient of determination (R^2) of four infiltration equations ranging from 0.84 to 0.96, indicating that these selected infiltration equations were able to well describe the infiltration process and the determined parameter values were accurate and reliable.

Model settings: for the plots with smooth and homogenous surfaces, the side length of each cell was set as 0.1 m, with 20 × 10 cells in total covering the whole plot. While for the more heterogeneous surfaces where rills developed, smaller cell size (0.01 m × 0.01 m) was used in order to capture the rill characteristics. The potential flow travel times were then calculated based on Eq. (6) using the method described in Section 2.3. The value of the 99% percentile was selected here as the time step for simulation. The resultant time step ranged from 0.044 s for plot 1 at 20° slope to 0.013 s for plot 6 at 40° slope.

4.3. Modeling results

RunCA was performed for the 20 mm/h and 70 mm/h rainfall events applied on all the plots at different slope gradients. The model performance was evaluated through the comparison of the predicted hydrographs with the measured runoff rates at certain time points, using both *EF* and *RMSE*. The resultant *EF* was on average 0.795 (0.033) for the 20 mm/h rainfall events, and was significantly correlated ($r = 0.446$, $P < 0.01$) to the R^2 for curve-fitting the infiltration equations, suggesting that a large portion of error in the simulated runoff rates was attributed to the error in estimating the infiltration parameters, instead of the inherent error of model itself. This is confirmed by the fact that when simulating runoff for the larger intensity (70 mm/h) rainfall events where infiltration played a less important role, the model performed much better, with the *EF* values significantly ($P < 0.01$) increased to 0.995 (0.001). Among all the simulations, the largest *RMSE* value was only 2.62 mm/h, and 80% of these values were less than 1.5 mm/h, suggesting a good model efficacy in predicting the runoff rates with time.

Correlation analysis showed that neither *EF* nor *RMSE* had significant correlation with the plot or slope gradient, indicating that the model performance did not vary much under different soil or topographic conditions. Three different flow-direction options were also compared, but no obvious difference was found, probably due to the relative simple slope profiles and homogenous surface conditions.

Fig. 5 shows the simulated flow maps at different time steps on a plot with rills development (plot 4 at 30% slope), during the 20 mm/h rainfall event and based on the Horton infiltration equation. It can be clearly seen that most water was flowing in the rills, while on the surface without rills, the water depth increased from the top to the bottom of the plot due to the accumulation of runoff water downslope. Besides, the runoff gradually expanded to a larger area and grew deeper with time due to the decreasing infiltration rate. All these results have indicated that the RunCA is able to describe both the spatial distribution and the temporal variation in the runoff process in this study.

4.4. Model sensitivity analysis

The above modeling results have suggested a close association between the simulated runoff and the infiltration parameters. To better understand the model response to the change in each of these parameters, sensitivity analysis was further performed. The 44 mm/h rainfall event applied on plot 2 at 30% slope was selected as a representative for this analysis. Then four 20% decrements and four 20% increments from the base infiltration parameter values (curve-fitting results) and the base Manning's n value were applied. In addition, the simulations based on eight cell sizes ranging from 0.01 m to 0.25 m of the cell side length were also performed, to evaluate the model sensitivity to the spatial resolution.

Two output parameters, total runoff Q_t and total infiltration amount INF_t, were used to evaluate the model responses. Fig. 6 shows that both Q_t and INF_t were more sensitive to A, K_s and i_f, which are all the parameters reflecting the steady infiltration rate, than the other infiltration parameters. Manning's n, the parameter influencing the flow velocity and thus time step, had almost no impact on the results. The model also showed very little response to the change of cell size (results are not shown here), probably due to the fact that the plot in this test was small and homogeneous.

5. Model validation with field measurements at the basin scale

Previous model validations by analytical solution and laboratory experiments have demonstrated the efficacy of the model in reproducing the basic runoff processes. Before applying it to the investigation of a real-world problem, one more step is required to test the model by field data under the natural conditions. There-

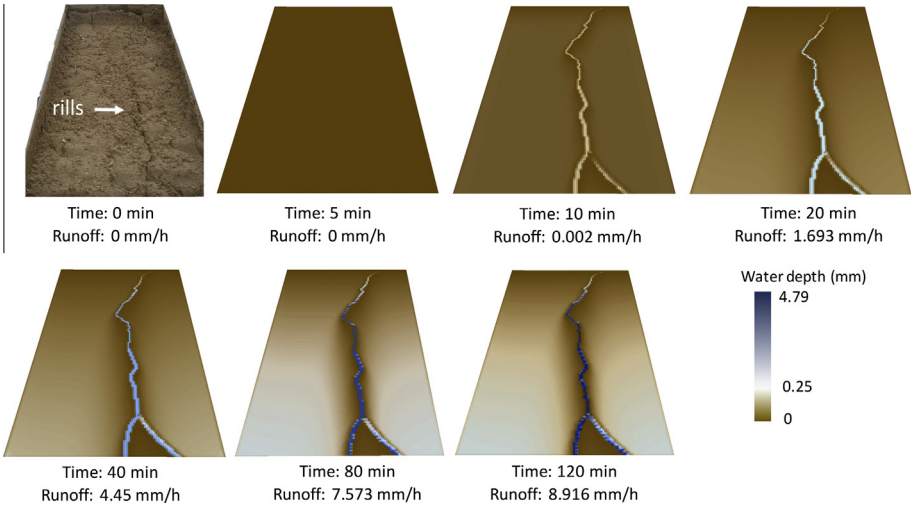

Fig. 5. Simulated flow maps at different time steps on laboratory plot 4 at 30% slope, 20 mm/h rainfall and based on Horton infiltration equation. The first flow map is a photo of plot surface at the initial condition.

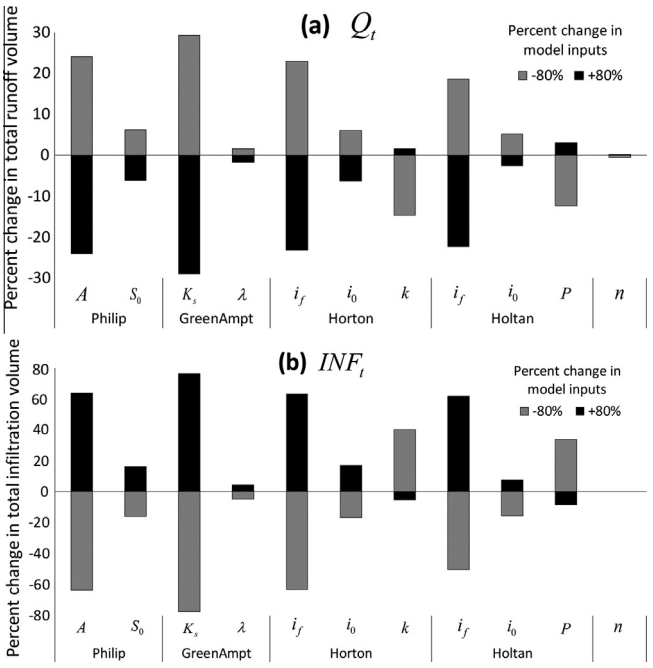

Fig. 6. Results for model sensitivity analysis performed on plot 2 at 30% slope and 44 mm/h rainfall intensity. Q_t and INF_t represents total runoff and total infiltration amount respectively, n represents Manning's roughness coefficient, while all the other symbols representing infiltration parameters are the same as those in Table 1.

fore the model performance was further evaluated by applying it to a representative natural basin.

5.1. Field data

Field data reported by Ritter (1992) were taken from the Pine Glen drainage basin located on rehabilitated surface mines in central Pennsylvania, to investigate its surface hydrology using our model RunCA. This basin (10.6 ha) was selected because it had well identified heterogeneous topographic and surface properties, which allowed the test of the model accuracy under complex conditions. A complete hydrology data set available in this basin is another advantage for model application. On the basis of vegetation type, land use, soil thickness and property, the basin could be divided into 5 different land units (Fig. 7a). More detailed descriptions of the surface characteristics of these land units are provided in Table S4 of the Supplementary material. For each unit, infiltration parameters were measured by infiltration tests conducted by Jorgensen and Gardner (1987) on 0.4 m × 0.1 m plots with a dripping-rainfall infiltrometer. In addition, a recording rain gauge and a water-level recorder housed in a cut-throat flume were installed to continuously measure the rainfall and runoff rates (Ritter, 1990).

5.2. Model inputs and settings

Cell elevation: the elevation values of spatial cells were derived from the basin DEMs (Fig. 7b and c), which were created from an original topography maps (Fig. S5-a in the Supplementary material) using ArcMap 10. The DEMs in different years after the rehabilitation showed different extents of the channel network development in this basin.

Rainfall: two observed rainfall events, with each in year 1 and 6 after the rehabilitation, were selected for model application. These rainfall events had temporally varied rainfall intensities, and thus were ideal for testing the model performance during complex rainfall conditions.

Interception: due to the lack of *LAI* information for this basin, the interception could not be calculated by Eq. (3). However, according to Ritter (1990), the maximum potential interception volume was only 0.5 mm in this basin (Table S6 in the Supplementary material) because of the low vegetation cover. Compared to the total rainfall amount (8.4 mm and 12.7 mm) used for simulations, the interception was negligible and thus not included in this simulation.

Infiltration: Based on the intermittent rainfall type and the available data, the modified Holtan infiltration equation (Table 1) was used in this simulation, with its measured input parameter values for each unit at different years shown in Table 3.

Manning's n: Different Manning's n values were used for the different land units and the channels, as suggested by Ritter (1990) and shown in Table 3.

Model settings: 1 m × 1 m cell size was set for the simulation, with 1.01×10^5 cells in total covering the whole basin. Based on the method introduced in Section 2.3, an estimated time step value of 1.37 s and 0.33 s, which equals to the calculated 99% percentile, was selected for the simulation in the year 1 and 6, respectively. The latter smaller value can be explained by the larger flow velocity in the developed channels.

5.3. Modeling results

The observed hydrograph for the chosen rainfall events, together with the simulated hydrographs based on the different flow-direction options, are demonstrated in Fig. 8. It can be seen that the predicted hydrographs based on the 4 + 4N option agree best with the measured hydrographs in both runoff events, with the *EF* values greater than 0.913 and *RMSE* values less than 0.183 mm/h. The hydrographs derived from the 4N option showed similar trends, however, they tend to underestimate the runoff rates. The reason for this can be found from the close examination of the flow maps as shown in Fig. 10. It can be seen that after 30 min of the rainfall event in year 6, there was still a portion of excess runoff trapped in the channels or small pits instead of flowing to the outlet, due to the limited flow directions to the cardinal neighbors of the 4N option. On the contrary, much less trapped water flow was observed in the according flow map derived from

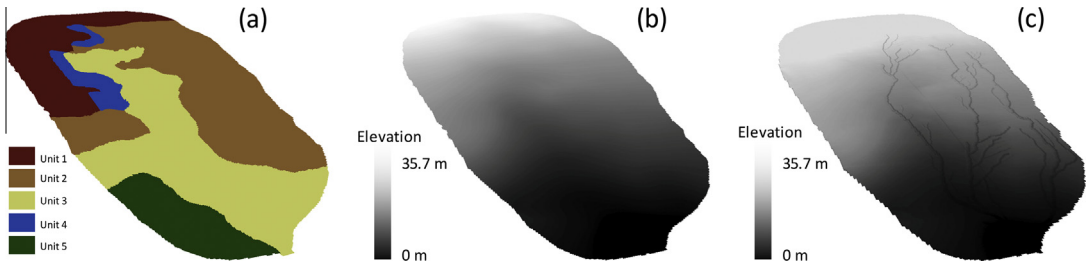

Fig. 7. Distribution of land units (a) of Pine Glen Basin, DEM in the year 1 (b) and the year 6 (c) after the rehabilitation.

Table 3
Infiltration Input Parameters and Manning's n for Runoff Simulations in Pine Glen Basin.[a]

Unit	i_f (mm/h)	i_0 (mm/h)	P	φ (%)	θ_0 (%)	FC (%)	D (mm)	Manning's n
Year 1								
1	60.00	64.50	0.55	43.00	6.45	21.50	100.00	0.25
2	10.00	64.50	1.00	30.00	4.50	15.00	25.00	0.075
3	10.00	64.50	1.00	30.00	4.50	15.00	25.00	0.075
4	10.00	64.50	1.00	30.00	4.50	15.00	25.00	0.075
5	10.00	64.50	1.00	30.00	4.50	15.00	25.00	0.075
Year 6								
1	60.00	64.50	0.55	43.00	6.45	21.50	100.00	0.25
2	9.00	63.50	10.00	27.00	4.05	13.50	25.00	0.05
3	20.00	70.40	1.00	30.00	4.50	15.00	25.00	0.075
4	22.00	62.00	4.00	43.00	6.45	21.50	25.00	0.05
5	13.20	71.00	10.00	28.00	4.20	14.00	25.00	0.25
Channels								0.05

[a] θ_0 represents the initial soil moisture, and all the other symbols are the same as those in Table 1.

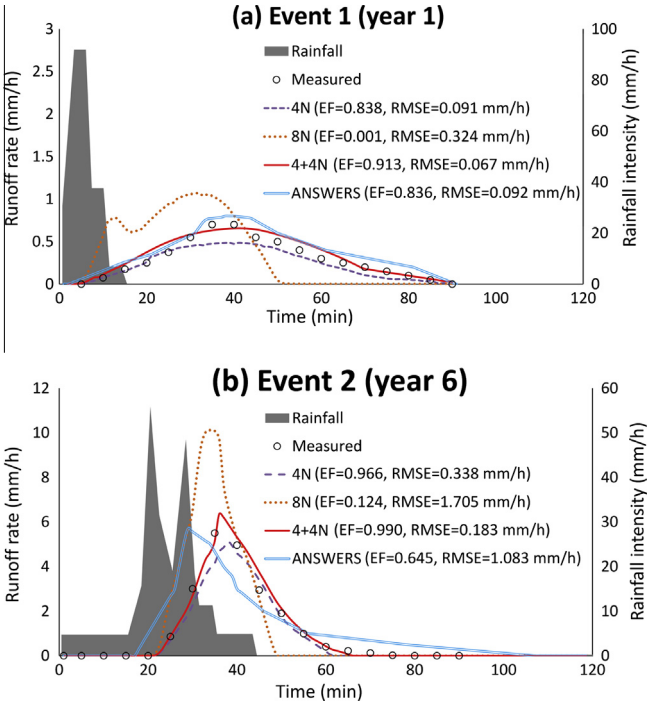

Fig. 8. Observed discharge rates and simulated hydrographs based on ANSWERS and different flow-direction options of RunCA for two rainfall events in the year 1 and 6 after rehabilitation.

the 4 + 4N option. The 8N flow-direction option failed here ($EF < 0.124$) in describing the shapes of the hydrographs, by overestimating the discharge rates and underestimating the durations of the runoff process. This may be attributed to the excessive flow divergence and unrealistic broadened flow pathways introduced by requiring water flow from a cell to all neighbor cells with smaller heights. These results are in line with our expectation that the 4 + 4N option is more accurate and realistic than the other two options as it controls the flow dispersion and at the same time maintains the eight possible flow directions. Therefore all the following model validation and sensitivity analysis are based on the results derived from this preferred option.

Event 1 occurred in the first year after the rehabilitation work, when no channel network was developed and relative low infiltration rates were observed on the newly established mine soils. Fig. 9 shows the simulated flow maps at different time steps in this runoff event. It can be seen that with the increasing rainfall intensity, runoff was generated in an expanding area and tended to flow to and accumulated in the central lower part of the basin, from where it further travelled to the outlet at the bottom of the basin. The runoff then disappeared gradually after the rainfall stopped. Due to the dominant overland flow process in this basin, the resultant hydrograph was characterized by low peak discharge rate, long lag time and gradual rising and recession limbs (Fig. 8a). All these characteristics were captured by the predicted hydrograph, indicating the model capacity in describing the overland flow.

The infiltration capacity of mine soil recovered gradually within six years following rehabilitation, and in the meantime the channel

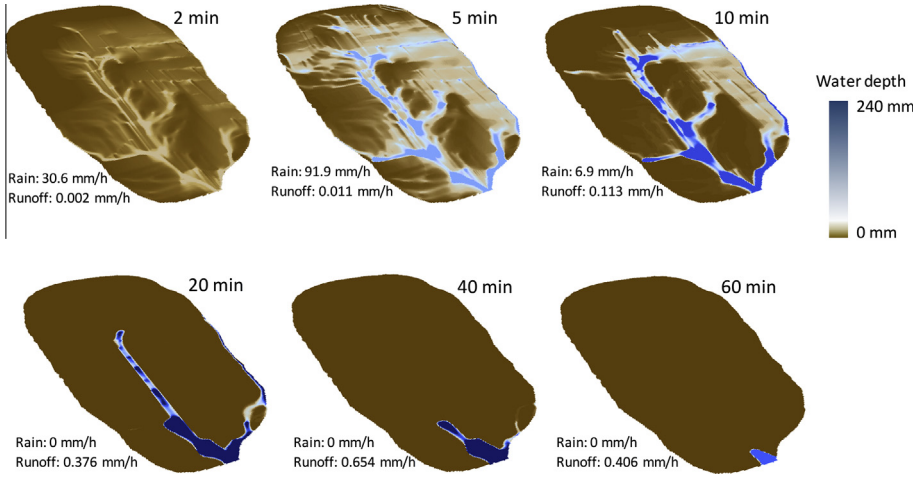

Fig. 9. Simulated flow maps at different time steps for rainfall event 1 in the year 1.

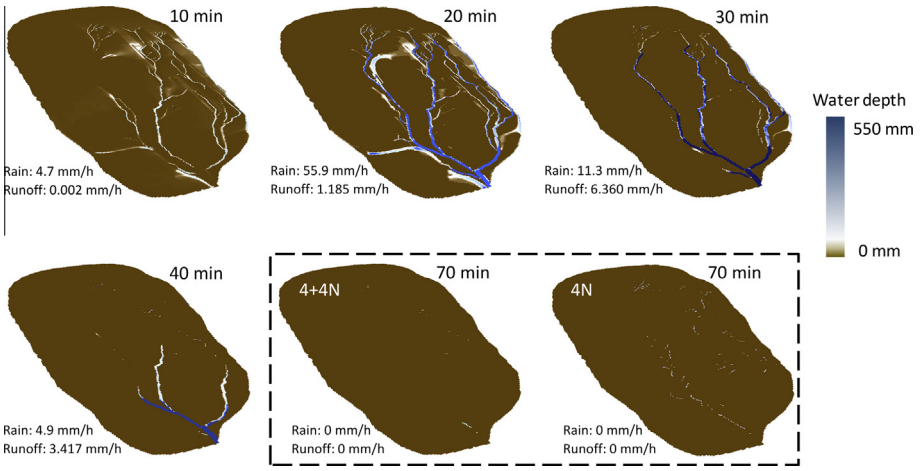

Fig. 10. Simulated flow maps at different time steps for rainfall event 2 in the year 6. The last two flow maps demonstrate the comparison of results derived from 4 + 4N and 4N flow direction options.

network initiation and maximum expansion in this basin occurred. The resultant simulated flow maps in the year 6 are shown in Fig. 10. It can be observed that the changes in runoff area and depth both responded quickly to the changes of rainfall intensity, and the channels captured and transmitted a majority of the produced runoff. Due to the dominant channelized flow process, which has higher efficiency for removal of surface runoff from the basin than the overland flow process, the observed hydrograph for this rainfall event exhibits a short lag time and time to peak, steep rising and recession limbs and high instantaneous peak discharge (Fig. 8b). Comparison of the hydrographs shows that the predicted and measured slopes of the rising limbs matched well, as well as the peak discharge values and the times to peak discharge. The observed falling limbs, however, showed a slightly longer lag time than the predicted one, probably due to the contribution of the sub-surface flow which is not considered in the current model, with the recovered infiltration capacity. Nevertheless, the general agreement of predicted and observed results demonstrated the model capacity in simulating the channelized flow.

The performance of RunCA were also compared to that of a well-known distributed physically based hydrologic model, ANSWERS (Beasley et al., 1980), in which the hydrologic response of any element in the basin is computed by an explicit, backward difference solution of the continuity equation, using Manning's equation as a stage-discharge relationship for both overland and channelized flow (Beasley and Huggins, 1981). More detailed descriptions of ANSWERS are provided in S3 of the Supplementary material. The model ANSWERS was chosen as its effectiveness in predicting surface runoff has been proven in a wide range of applications (Amin, 1982; Razavian, 1990; Sichani and Engel, 1990; Singh et al., 2006). Its performance was also found comparable to some other hydrologic models (Bhuyan et al., 2002; Borah and Bera, 2004; Walling et al., 2003). This model was also selected as it enabled the incorporation of the same infiltration model (i.e., the Holtan model) as RunCA and thus a similar set of input parameters, including infiltration parameters and Manning's n (Table 3 and Table S6 in the Supplementary material), were used for both models. This allows the comparison of model performance by excluding the influence of errors in deriving the parameter values. The detailed information related to the spatial representation of the basin by square grids, and the input parameter values used for simulations by ANSWERS for these two rainfall events can be found in Fig. S5-b and Table S6 of the Supplementary material, respectively. Comparison of simulation results showed that there was no significant difference in the performance of ANSWERS and RunCA in the simulation of the hydrograph of rainfall event 1, although RunCA had a slightly larger *EF* value a smaller RMSE value (Fig. 8a). However, ANSWERS produced obvious bias in simulating the hydrograph of rainfall event 2 by underestimating the lag time of runoff production following the rainfall (Fig. 8b), while RunCA agreed much better with the observed discharge rates. These results indicated an improvement of simulation accuracy by using RunCA instead of ANSWERS in this case study.

5.4. Model sensitivity analysis

To better understand the model response to the change in each input parameter and model setting, sensitivity analysis was performed, using runoff event 2. Three runoff output parameters that describe hydrographs and two infiltration output parameters (Fig. 11) were used to evaluate the model responses. The infiltration parameter and Manning's n values for year 6 in Table 3 were selected as the base values. Then four 20% decrements and four 20% increments from these base values were applied for the sensitivity analysis. In addition, the simulations based on eight cell sizes ranging from 0.1 to 10 times of its original value of the cell side length were also performed.

Fig. 11 shows the model sensitivity analysis results, which are expressed as the percentage changes from the base output values. It can be found that the output parameters were all significantly sensitive to the change in the final steady infiltration rate i_f, indicating the importance of i_f in this model. In addition, both peak discharge rate Q_p and time to peak T_p, the parameters determining the hydrograph shapes, were greatly influenced by the Manning's n, due to its role in changing the flow velocity according to Eq. (5). The total drainage amount DR_t was also very sensitive to φ, *FC* and *D*, which is not surprising because they are all parameters for the modified Holtan equation as shown in Table 1. The change of spatial resolution to different directions had different impacts on the outputs. When reducing the cell side length to 0.1 m, the results were not significantly affected. But when increasing it gradually to 10 m, the total discharge Q_t and Q_p were greatly reduced, while T_p and the total infiltration INF_t were increased. This can be due to the reason that large cell sizes lead to the loss of micro-topographic details and the channel information, and thus result in inaccurate outputs.

6. Conclusions

A CA-based model (RunCA) has been developed to simulate the production and distribution of surface runoff. The efficacy of the

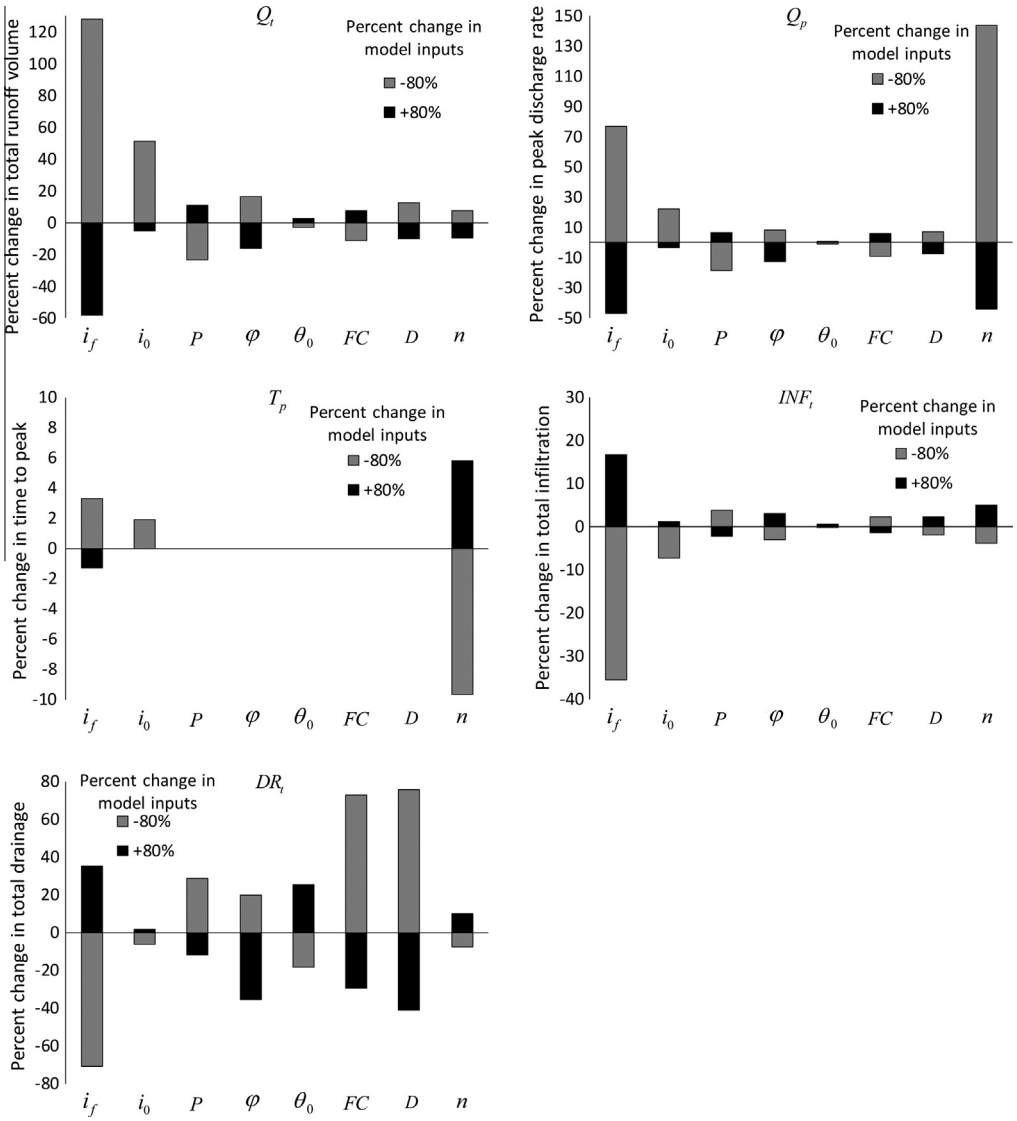

Fig. 11. Model sensitivity analysis results at the basin scale. Q_t, Q_p and T_p represents total discharge, peak discharge and time to peak discharge respectively, INF_t and DR_t represents total infiltration and total drainage respectively, n represents Manning's roughness coefficient, while all the other symbols representing infiltration parameters are the same as those in Table 1.

model was initially validated by three steps. The comparison with the analytical solution proved the effectiveness of the calculation algorithms of RunCA in simulating the runoff distribution. The results of laboratory experiments on small plots showed that the model predicted the hydrographs with the average *EF* above 0.90 and *RMSE* below 0.50 mm/h. Its performance was not affected by varied soil or topographic conditions, but was most sensitive to the input final steady infiltration rate of soil, which could be measured directly in the field. Validation by field measurements at a basin showed that the 4 + 4N flow-direction option provided the best agreement between the simulated and measured hydrographs. The spatial distribution and temporal variation of the runoff process could also be described by RunCA, as reflected in the flow maps. RunCA showed better performance compared to ANSWERS in predicting the hydrographs in this case study. In addition to the steady infiltration rate, the modeling results at this large scale were sensitive to the Manning's n because of the changed flow velocity, as well as to the setting of cell size due to the loss of topographic details.

This study applied a new technique, Cellular Automata, for runoff modeling. The cell structure of RunCA, which enables its integration with GIS, can provide an accurate and easy representation of the study area. Linking ground-truthed data of hydrological properties with remote sensed data as model inputs broadens the range of options of applications for this model. The simultaneous update of states of all the spatial cells at multiple time steps enables the model to describe the spatially and temporally varied runoff behaviors. Compared to the traditional kinematic wave and diffusion wave methods, which only simulate the one-dimensional runoff process based on some simplifying assumptions, RunCA is expected to better capture the spatial variations in flow distribution by simulating the runoff process in two dimensions from local to global. The simple transition rules used in RunCA greatly reduced the complexity in computation by some advanced numerical techniques (e.g., 2-D diffusion wave method), as there is no need to solve any complex equations of continuity or momentum. These CA transition rules are also considered to be more realistic than the DEM-based routing algorithms as they determine the water distribution based on the water surface elevations instead of the land surface elevations. This model would be a further step based on the existing CA runoff models by considering the spatially varied flow velocities, introducing a more realistic 4

+ 4N flow-direction algorithm and incorporating physically measurable hydrologic principles (e.g., infiltration characteristic) when determining the runoff production. Besides, instead of restricting to a certain spatial or temporal scale, RunCA is developed as a universal tool to be applied in different spatial scales for both event-based and long-term simulations.

At current stage RunCA focuses only on the simulation of infiltration-excess runoff (Hortonian runoff) processes, thus it may produce some inaccurate results when applying it to the large scale study area where different runoff generation mechanisms (e.g., saturation-excess runoff or subsurface runoff) are dominant. For the validations in this study, the impacts of vegetation (e.g. interception) on surface runoff were not included due to lack of appropriate information or type of test. This needs to be further evaluated. Here the validations of the model concentrate on comparisons of hydrographs and flow maps. However, some other important variables, such as the height of the water film during runoff and the velocity of the overland flow have not been investigated due to the difficulties in measurement. More advanced techniques can be employed for this purpose in further studies. As the main purpose of this paper was to focus on the introduction of the model, the developed model was only tested in limited case studies using limited rainfall events. Nevertheless, based on the results there is promising potential for successfully applying this model and evaluating its performance to other spatial or temporal scales and under more complex conditions.

Acknowledgements

The authors thank Wei Gu for the guidance in experimental design and data analysis for the rainfall simulation experiments. Thank all the reviewers for their valuable comments and constructive feedback on improving this paper.

Appendix A. Supplementary material

Supplementary data associated with this article can be found, in the online version, at http://dx.doi.org/10.1016/j.jhydrol.2015.09.003.

References

Abbott, M.B., Bathurst, J.C., Cunge, J.A., O'Connell, P.E., Rasmussen, J., 1986. An introduction to the European Hydrological System – Systeme Hydrologique Europeen, "SHE", 2: Structure of a physically-based, distributed modelling system. J. Hydrol. 87 (1–2), 61–77.

Amin, S., 1982. Modeling of phosphorous transport in surface runoff from agriculture watersheds. PhD Thesis Thesis, Purdue University, West Lafayette, USA.

Aron, G., 1992. Adaptation of Horton and SCS infiltration equations to complex storms. J. Irrigation Drain. Eng. 118 (2), 275–284.

Aston, A.R., 1979. Rainfall interception by eight small trees. J. Hydrol. 42 (3–4), 383–396.

Bauer, S.W., 1974. A modified Horton equation for infiltration during intermittent rainfall. Hydrol. Sci. Bull. 19 (2), 219–225.

Beasley, D.B., Huggins, L.F., 1981. ANSWERS Users Manual. Environmental Protection Agency, Chicago, U.S, 53 pp.

Beasley, D.B., Huggins, L.H., Monke, E.J., 1980. ANSWERS: a model for watershed planning. Trans. Am. Soc. Agric. Eng. 23, 938–944.

Bhuyan, S.J., Kalita, P.K., Janssen, K.A., Barnes, P.L., 2002. Soil loss predictions with three erosion simulation models. Environ. Modell. Software 17 (2), 135–144.

Borah, K.D., Bera, M., 2004. Watershed-scale hydrologic and nonpoint-source pollution models: review of applications. Trans. ASAE 47 (3), 789–803.

Cervarolo, G., Mendicino, G., Senatore, A., 2011. Coupled vegetation and soil moisture dynamics modeling in heterogeneous and sloping terrains. Vadose Zone J. 10 (1), 206–225.

Chaudhry, M.H., 1993. Open Channel Flow. Prentice Hall, Englewood Cliffs, NJ.

Chow, V.T., Maidment, D.R., Mays, L.W., 1988. Applied Hydrology. McGraw-Hill, New York.

Costa-Cabral, M.C., Burges, S.J., 1994. Digital Elevation Model Networks (DEMON): a model of flow over hillslopes for computation of contributing and dispersal areas. Water Resour. Res. 30 (6), 1681–1692.

Coulthard, T.J., Kirkby, M.J., Macklin, M.G., 2000. Modelling geomorphic response to environmental change in an upland catchment. Hydrol. Process. 14 (11–12), 2031–2045.

De Roo, A.P.J., Wesseling, C.G., Ritsema, C.J., 1996. LISEM: a single-event physically based hydrological and soil erosion model for drainage basins. I: Theory, input and output. Hydrol. Process. 10 (8), 1107–1117.

Erskine, R.H., Green, T.R., Ramirez, J.A., MacDonald, L.H., 2006. Comparison of grid-based algorithms for computing upslope contributing area. Water Resour. Res. 42 (9), W09416.

Fairfield, J., Leymarie, P., 1991. Drainage networks from grid digital elevation models. Water Resour. Res. 27 (5), 709–717.

Favis-Mortlock, D., 1998. A self-organizing dynamic systems approach to the simulation of rill initiation and development on hillslopes. Comput. Geosci. 24 (4), 353–372.

Feldman, A.D., 1995. HEC-1 flood routing package. In: Singh, V.J. (Ed.), Computer Models of Watershed Hydrology. Water Resources Publication, Highlands Ranch, Colorado, pp. 119–150.

Folino, G., Mendicino, G., Senatore, A., Spezzano, G., Straface, S., 2006. A model based on cellular automata for the parallel simulation of 3D unsaturated flow. Parallel Comput. 32 (5–6), 357–376.

Green, W.H., Ampt, C.A., 1911. Studies on soil physics I. The flow of air and water through soils. J. Agric. Sci. 5, 1–24.

Gregorio, S.D., Serra, R., 1999. An empirical method for modelling and simulating some complex macroscopic phenomena by cellular automata. Future Gener. Comput. Syst. 16 (2–3), 259–271.

Haan, C.T., Johnson, H.P., Brakensiek, D.L., 1982. Hydrologic Modeling of Small Watersheds. American Society of Agricultural Engineers, Michigan.

Holtan, H.N., 1961. A concept of Infiltration Estimates in Watershed Engineering. U. S. Department of Agricultural Service, Washington, DC.

Horton, R.E., 1940. An approach towards a physical interpretation of infiltration capacity. Soil Sci. Soc. Am. Proc. 5, 399–417.

Huggins, L.F., Monke, E.J., 1966. The mathematical simulation of the hydrology of small watersheds, Water Resources Research Center, Purdue University.

Huggins, L.F., Monke, E.J., 1968. A mathematical model for simulating the hydrologic response of a watershed. Water Resour. Res. 4 (3), 529–539.

Jorgensen, D.W., Gardner, T.W., 1987. Infiltration capacity of disturbed soils: temporal change and lithologic control. Water Resour. Bull 23, 1161–1172.

Knisel, W.G., 1980. CREAMS. A field scale model for chemicals, runoff and erosion from agricultural management systems. United States Department of Agriculture Conservation Research Report, vol. 26.

Laflen, J.M., Lane, L.J., Foster, G.R., 1991. WEPP: a new generation of erosion prediction technology. J. Soil Water Conserv. 46 (1), 34–38.

Ma, T., Zhou, C.-H., Cai, Q.-G., 2009. Modeling of hillsloperunoff and soil erosion at rainfall events using cellular automata approach. Pedosphere 19 (6), 711–718.

MacArthur, R., DeVries, J.J., 1993. Introduction and Application of Kinematic Wave Routing Techniques Using HEC-1, Hydrologic Engineering Centre.

Mendicino, G., Pedace, J., Senatore, A., 2013. Cellular automata based modeling for the assessment of ecohydrological dynamics at the hillslope scale: preliminary results. Procedia Environ. Sci. 19, 311–320.

Mendicino, G., Senatore, A., Spezzano, G., Straface, S., 2006. Three-dimensional unsaturated flow modeling using cellular automata. Water Resour. Res. 42 (11), W11419.

Morgan, R.P.C., Quinton, J.N., Smith, R.E., Govers, G., Poesen, J.W.A., 1998a. The European Soil Erosion Model (EUROSEM): Documentation and User Guide. Cranfield University, Silsoe College.

Morgan, R.P.C. et al., 1998b. The European Soil Erosion Model (EUROSEM): A dynamic approach for predicting sediment transport from fields and small catchments. Earth Surf. Proc. Land. 23, 527–544.

Murray, A.B., Paola, C., 1994. A cellular model of braided rivers. Nature 371 (1), 54–57.

Nash, J.E., Sutcliffe, J.V., 1970. River flow forecasting through conceptual models Part I — a discussion of principles. J. Hydrol. 10 (3), 282–290.

O'Callaghan, J.F., Mark, D.M., 1984. The extraction of drainage networks from digital elevation data. Comput. Vision Graphics Image Process. 28 (3), 323–344.

Parsons, J.A., Fonstad, M.A., 2007. A cellular automata model of surface water flow. Hydrol. Process. 21 (16), 2189–2195.

Philip, J.R., 1957. The theory of infiltration: 1. The infiltration equation and its solution. Soil Sci. 83, 345–357.

Quinn, P., Beven, K., Chevallier, P., Planchon, O., 1991. The prediction of hillslope flow paths for distributed hydrological modelling using digital terrain models. Hydrol. Process. 5 (1), 59–79.

Ravazzani, G., Rametta, D., Mancini, M., 2011. Macroscopic cellular automata for groundwater modelling: a first approach. Environ. Modell. Software 26 (5), 634–643.

Razavian, D., 1990. Hydrologic responses of an agricultural watershed to various hydrologic and management conditions. JAWRA J. Am. Water Resour. Assoc. 26 (5), 777–785.

Renard, K.G., Foster, G.R., Weesies, G.A., McCool, D.K., Yoder, D.C., 1997. Predicting soil erosion by water: a guide to conservation planning with the Revised Universal Soil Loss Equation (RUSLE), Agriculture Handbook. U.S. Department of Agriculture, Washington, D. C.

Rinaldi, P.R., Dalponte, D.D., Vénere, M.J., Clausse, A., 2007. Cellular automata algorithm for simulation of surface flows in large plains. Simul. Model. Pract. Theory 15 (3), 315–327.

Ritter, J.B., 1990. Surface Hydrology of Drainage Basins Disturbed by Surface Mining and Reclamation, Central Pennsylvania. Pennsylvania State University, University Park, PA, 182 pp.

Ritter, J.B., 1992. Application of field infiltration data to hydrologic model parameterization: an example from drainage basins disturbed by surface mining. J. Hydrol. 134 (1–4), 173–202.
Rojas, R., Julien, P., Johnson, B., 2003. Reference Manual for A 2-Dimensional Rainfall-Runoff and Sediment Model, Colorado State University.
Schmidt, J., Werner, M.v., Michael, A., 1999. Application of the EROSION 3D model to the CATSOP watershed, The Netherlands. CATENA 37 (3–4), 449–456.
Sichani, S.A., Engel, B.A., 1990. Prediction of runoff and sediment from agricultural watersheds by a mathematical model: II. Mathematical simulation. Iran Agric. Res. 9, 1–16.
Singh, R., Tiwari, K.N., Mal, B.C., 2006. Hydrological studies for small watershed in India using the ANSWERS model. J. Hydrol. 318 (1–4), 184–199.
Singh, V.P., 1996. Kinematic Wave Modeling in Water Resources: Surface-Water Hydrology. John Wiley, New York, 1399 pp.
Smith, R.E., 1981. A kinematic model for surface mine sediment yield. Trans. ASAE 24, 1508–1514.
Swensson, M.T., 2003. Refinements on a GIS-Based, Spatially Distributed Rainfall-Runoff Model for a Small Watershed. University of Pittsburgh, 125 pp.
Tarboton, D.G., 1997. A new method for the determination of flow directions and upslope areas in grid digital elevation models. Water Resour. Res. 33 (2), 309–319.
U.S. Department of Agriculture, S.C.S., 1972. Hydrology, SCS National Engineering Handbook. Section 4. U.S. Gov. Print. Office, Washington, D.C.
Vieux, B.E., 1991. Geographic information systems and non-point source water quality and quantity modelling. Hydrol. Process. 5 (1), 101–113.
Von Hoyningen-Huene, J., 1981. Die Interzeption des Niederschlags in landwirtschaftlichen Pflanzenbeständen. Arbeitsbericht Deutscher Verband für Wasserwirtschaft und Kulturbau, DVWK, Braunschweig, 63 pp.
Von Neumann, J., 1966. Theory of Self Reproducing Automata. University of Illinois Press Champaign, IL, USA.
Walling, D.E., He, Q., Whelan, P.A., 2003. Using 137Cs measurements to validate the application of the AGNPS and ANSWERS erosion and sediment yield models in two small Devon catchments. Soil Tillage Res. 69 (1–2), 27–43.
Wang, S., Roache, P., Schmalz, R., Jia, Y., Smith, P., 2009. Verification and Validation of 3D Free-Surface Flow Models. American Society of Civil Engineers.
Wang, S., Wu, W., 2004. River sedimentation and morphology modeling – the state of the art and future development, Proceedings of the Ninth International Symposium on River Sedimentation, Yichang, China, pp. 71–94.
Wischmeier, W.H., Smith, D.D., 1978. Predicting rainfall erosion losses: A guide to conservation planning, Agriculture Handbook. U.S. Department of Agriculture, Washington, D.C.
Wolfram, S., 1984. Computation theory of cellular automata. Commun. Math. Phys. 96 (1), 15–57.
Young, R.A., Onstad, C.A., Bosch, D.D., Anderson, W.P., 1989. AGNPS: A nonpoint-source pollution model for evaluating agricultural watersheds. J. Soil Water Conserv. 44 (2), 168–173.